

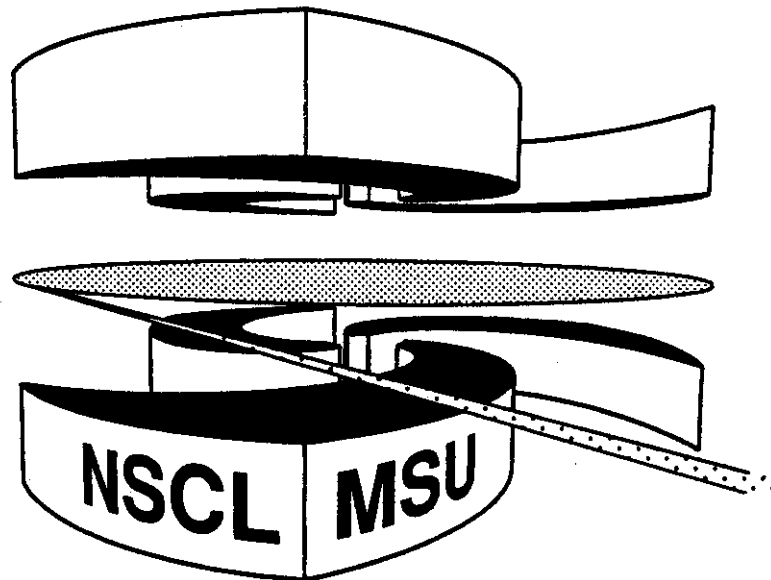


Michigan State University

National Superconducting Cyclotron Laboratory

**OBSERVATION OF LIFETIME EFFECTS IN TWO-PROTON
CORRELATIONS FOR WELL-CHARACTERIZED SOURCES**

**M.A. LISA, C.K. GELBKE, P. DECOWSKI,
W.G. GONG, E. GUALTIERI, S. HANNUSCHKE,
R. LACEY, T. LI, W.G. LYNCH, G.F. PEASLEE,
S. PRATT, T. REPOSEUR, A.M. VANDERMOLEN,
G.D. WESTFALL, J. LEE, and S.J. YENNELLO**



Observation of Lifetime Effects in Two-Proton Correlations for Well-Characterized Sources

M.A. Lisa, C.K. Gelbke, P. Decowski¹, W.G. Gong², E. Gualtieri, S. Hannuschke, R. Lacey³, T. Li, W.G. Lynch, G.F. Peaslee, S. Pratt, T. Reposeur⁴, A.M. Vander Molen, G.D. Westfall, J.Yee, and S.J. Yennello⁵

*National Superconducting Cyclotron Laboratory
and Department of Physics and Astronomy
Michigan State University, East Lansing, MI 48824, USA*

Abstract

Differences between longitudinal and transverse two-proton correlation functions, consistent with finite **lifetime** effects, are observed for central $^{36}\text{Ar} + ^{45}\text{Sc}$ collisions at $E/A=80$ MeV. The correlations between two protons emitted with low total momenta are consistent with emission from a source of Gaussian radius $r_0 \approx 3.5 \pm 0.5$ fm and characteristic lifetime $\tau \approx 70 \pm 30$ fm/c.

PACS number: 25.70.Pq

¹Present address: Department of Physics, Smith College, Northampton, MA

²Present address: Lawrence Berkeley Laboratory, Berkeley, CA 94720

³Present address: Department of Chemistry, State University of New York, Stony Brook, NY 11776

⁴Present address: Laboratoire de Physique Nucléaire, Université de Nantes, Nantes Cedex 03, France

⁵Present address: Cyclotron Institute, Texas A&M University, College Station, TX 77843

Two-proton correlation functions at small relative momenta probe the space-time geometry of the emitting system, because the magnitude of nuclear and Coulomb final-state interaction and antisymmetrization effects depends on the spatial separation of the emitted particles [1-28]. The attractive S-wave nuclear interaction leads to a pronounced maximum in the correlation function at relative momentum $q \approx 20$ MeV/c. This maximum decreases for increasing source dimensions and/or emission time-scales. The Coulomb interaction and antisymmetrization produce a minimum at $q \approx 0$. Non-spherical phase-space distributions, predicted for long-lived emission sources, can lead to a dependence of the two-proton correlation function on the direction of the relative momentum [13,23]. Until now, however, such directional dependences have not yet been observed unambiguously [16,18,21,24,25,28], possibly because a clear characterization of emission sources was not achieved in previous experiments [28,29]. In this paper, we present a clear observation of a difference between longitudinal and transverse two-proton correlation functions in an experiment with full event characterization. The observed difference can be attributed to the finite lifetime of the emitting system.

The experiment was performed at the National Superconducting Cyclotron Laboratory at Michigan State University. A beam of ^{36}Ar ions at $E/A=80$ MeV incident energy bombarded a ^{45}Sc target of areal density 10 mg/cm². The beam intensity was typically 3×10^8 particles/sec. Charged particles were measured in the MSU 4π Array [30], which consisted of 209 plastic ΔE -E phoswich detectors covering polar angles between 7° and 158° in the laboratory frame. Particles stopping in the slow (E) plastic scintillators of this array were identified by their particle type and energy; the energy calibrations for these detectors are accurate to approximately 10%. One of the hexagonal modules of the 4π Array, located at

38° in the lab frame, was replaced by a 56-telescope high-resolution hodoscope [24,31,32]. Each ΔE -E telescope of the hodoscope consisted of a 300- μm -thick Si detector backed by a 10-cm-long CsI(Tl) detector and subtended a solid angle of $\Delta\Omega = 0.37$ msr. The nearest-neighbor separation between telescopes was $\Delta\theta = 2.6^\circ$, and the energy resolution of each telescope was about 1% for 60 MeV protons. During the experiment, both two-proton coincidence and singles events in the hodoscope were recorded in coincidence with the corresponding data from the 4π Array.

The problem of identifying finite-lifetime effects is illustrated in Fig. 1. The figure depicts phase space distributions of protons emitted towards the detector at $\theta_{\text{lab}} = 38^\circ$ for a source at rest in the laboratory (part a) and for a source at rest in the center-of-momentum system of projectile and target ($v_{\text{source}} = 0.18c$, part b). We assumed a spherical source of 7 fm diameter and 70 fm/c lifetime emitting protons of momentum 250 MeV/c.

For emission from a source at rest, the phase space distribution of particles moving with a fixed velocity $v_{p,\text{lab}} = v_{\text{emit}}$ towards the detector exhibits an elongated shape [13,24,33] oriented parallel to $v_{p,\text{lab}}$. A source of lifetime τ appears elongated by an incremental distance $\Delta s \approx v_{\text{emit}} \cdot \tau = v_{p,\text{lab}} \cdot \tau$. Correlation functions for relative momenta $q \perp v_{p,\text{lab}}$ reflect a stronger Pauli-suppression, and hence a reduced maximum at $q \approx 20$ MeV/c, than those for $q \parallel v_{p,\text{lab}}$ [13,23,24,33].

Previous analyses [2,16,21,24,25] compared the shapes of correlation functions selected by cuts on the relative angle $\psi_{\text{lab}} = \cos^{-1}(q \cdot P / qP)$ between q and $P = p_1 + p_2 \approx 2mv_{p,\text{lab}}$, where p_1 and p_2 are the laboratory momenta of the two protons and q is the momentum of relative motion. Such analyses are optimized to detect lifetime effects of sources stationary in the laboratory system,

but they can fail to detect lifetime effects for non stationary sources. For the specific case illustrated in Fig. 1b, the source dimensions parallel and perpendicular to $\mathbf{v}_{p,lab}$ are very similar, and no significant differences are expected for the corresponding longitudinal and transverse correlation functions.

For a source of known velocity, the predicted lifetime effect is detected most clearly if longitudinal and transverse correlation functions are selected by cuts on the angle $\psi_{source} = \cos^{-1}(\mathbf{q}' \cdot \mathbf{P}' / q'P')$, where the primed quantities are defined in the rest frame of the source. (In Fig. 1b, the source dimensions should be compared in directions parallel and perpendicular to \mathbf{v}_{emit} .) Such analyses can only be carried out for emission from well characterized sources [28]. In the following, we corroborate these qualitative arguments by our experimental data.

The experimental two-proton correlation function $1+R(q)$ is defined in terms of the two-proton coincidence yield $Y_2(\mathbf{p}_1, \mathbf{p}_2)$ and the proton singles yield $Y_1(\mathbf{p})$:

$$\Sigma Y_2(\mathbf{p}_1, \mathbf{p}_2) = C [1+R(q)] \Sigma Y_1(\mathbf{p}_1)Y_1(\mathbf{p}_2), \quad (1)$$

where q is the (invariant) magnitude of the relative momentum four-vector. For a given experimental gating condition, the sums on each side of Eq. (1) extend over all proton energies and detector combinations of the 56-element hodoscope corresponding to each q -bin. The normalization constant C is determined by the requirement that $R(q)$ vanish for large q .

Figure 2 shows longitudinal and transverse two-proton correlation functions for central $^{36}\text{Ar} + ^{45}\text{Sc}$ collisions at $E/A = 80$ MeV selected by appropriate cuts [34] on the total transverse energy detected in the 4π Array. In a geometrical picture [34,35], the applied cuts correspond to reduced impact parameters [35] of $b/b_{max} = 0 - 0.36$. Longitudinal (solid points) and transverse (open points) correlation functions were defined by cuts on the angle $\psi = \cos^{-1}(\mathbf{q} \cdot \mathbf{P} / qP) = 0^\circ - 50^\circ$ and $80^\circ - 90^\circ$, respectively. (The normalization constant C in Eq. 1 is

independent of ψ .) To maximize lifetime effects and reduce contributions from the very early stages of the reaction, the coincident proton pairs were selected by a low-momentum cut [34] on the total laboratory momentum, $P = 400\text{-}600$ MeV/c. The top panel shows correlation functions for which the angle ψ was defined in the center-of-momentum frame of projectile and target ($\psi = \psi_{\text{source}}$); for central collisions of two nuclei of comparable mass, this rest frame should be close to the rest frame of the emitting source. The bottom panel shows correlation functions for which the angle ψ was defined in the laboratory frame ($\psi = \psi_{\text{lab}}$).

Consistent with the qualitative arguments presented in Fig. 1, a clear difference between longitudinal and transverse correlation functions is observed for cuts on ψ_{source} (top panel of Fig. 2), but not for cuts on ψ_{lab} (bottom panel of Fig. 2). The clear suppression of the transverse correlation function with respect to the longitudinal correlation function observed in the top panel in Fig. 2 is consistent with expectations for emission from a source of finite lifetime [13,23,24,33]. The solid and dashed curves in the top panel of Fig. 2 depict calculations for emission from a spherical Gaussian source of radius parameter $r_0 = 3.5$ fm and lifetime $\tau = 70$ fm/c, see also Eq. 2 below. The data in Fig. 2 represent the first clear experimental evidence of this predicted lifetime effect.

Clean characterization of a relatively well defined source frame appears crucial. Two-proton correlation functions selected by more peripheral cuts did not exhibit any differences between longitudinal and transverse correlation functions, irrespective whether the cuts on ψ were defined in the laboratory, the center-of-momentum frame for the $^{36}\text{Ar} + ^{45}\text{Sc}$ system, or the projectile rest frame. Indeed, for such collisions no single unique source velocity may exist, and more sophisticated analysis techniques may be necessary to exploit directional dependences of two-proton correlation functions. More interestingly, even for

central collisions no significant difference between longitudinal and transverse correlation functions was observed for protons selected by cuts on large total momenta, $P \geq 700$ MeV/c. These very energetic protons appear to be emitted on a very fast time scale and/or at such an early stage of the reaction where the concept of emission from a single source does not apply.

For a more quantitative analysis, we performed calculations assuming a simple family of sources of lifetime τ and spherically symmetric Gaussian density profiles, moving with the center-of-momentum frame of reference. Energy and angular distributions of the emitted protons were selected by randomly sampling the experimental yield $Y(\mathbf{p})$. Specifically, the single particle emission functions [23,24] were parametrized as

$$g(\mathbf{r}, \mathbf{p}, t) \propto \exp(-r^2/r_0^2 - t/\tau) \cdot Y(\mathbf{p}). \quad (2)$$

In Eq. 2, \mathbf{r}, \mathbf{p} , and t refer to the rest frame of the source. Phase-space points generated in the rest frame of the source were Lorentz boosted into the laboratory frame, and the two-proton correlation function was obtained by convolution with the two-proton relative wavefunction, see refs. [13,23,24] for details.

Transverse and longitudinal correlation functions were calculated for the range of parameters $r_0 = 2.5 - 6.5$ fm and $\tau = 0 - 200$ fm/c. For each set of parameters, the agreement between calculated and measured longitudinal and transverse correlation functions was evaluated by determining the value of χ^2/ν (chi-squared per degree of freedom) in the peak region, $q = 15 - 30$ MeV/c. A contour plot of χ^2/ν as a function of r_0 and τ is given in Fig. 3. Good agreement between calculations and data is obtained in a valley roughly bounded by $(r_0 = 4.5$ fm, $\tau = 40$ fm/c) and $(r_0 = 3.0$ fm, $\tau = 110$ fm/c). The extracted emission

timescales of 40 - 110 fm/c are consistent with those predicted by microscopic transport calculations [22-24].

In conclusion, we have presented the first conclusive measurement of a difference between longitudinal and transverse two-proton correlation functions which is consistent with a predicted [13,23,24,33] finite-lifetime effect. For the identification of this effect, determination of the source rest frame was shown to be essential. For central nucleus-nucleus collisions at intermediate energies, such clear-cut event characterization appears possible by impact parameter selection, but for peripheral collisions more sophisticated techniques may be needed to exploit the directional information contained in two-proton correlation functions. The observation and exploitation of directional dependences of two-particle correlation functions promises to open new possibilities of probing the space-time characteristics of reaction zones formed in intermediate and high-energy nucleus-nucleus collisions with much higher sensitivity than achieved in previous investigations.

This work was supported by the National Science Foundation under Grant No. PHY-9214992.

References

1. S.E. Koonin, Phys. Lett. **B70**, 43 (1977).
2. F. Zarbaksh et al., Phys. Rev. Lett. **46**, 1268 (1981).
3. W.G. Lynch et al., Phys. Rev. Lett. **51**, 1850 (1983).
4. W.G. Lynch et al., Phys. Rev. Lett. **52**, 2302 (1984).
5. H. A. Gustafsson et al., Phys. Rev. Lett. **53**, 544 (1984).
6. C.B. Chitwood et al., Phys. Rev. Lett. **54**, 302 (1985).
7. J. Pochodzalla et al., Phys. Lett. **B174**, 36 (1986).
8. A. Kyanowski et al., Phys. Lett. **B181**, 43 (1986).
9. J. Pochodzalla et al., Phys. Rev. **C35**, 1695 (1987).
10. Z. Chen et al., Phys. Rev. **C36**, 2297 (1987).
11. Z. Chen et al., Phys. Lett. **B186**, 280 (1987).
12. Z. Chen et al., Nucl. Phys. **A473**, 564 (1987).
13. S. Pratt and M.B. Tsang, Phys. Rev. **C36**, 2390 (1987).
14. P. Depieux et al., Phys. Lett. **B200**, 17 (1988).
15. D. Fox et al., Phys. Rev. **C38**, 146 (1988).
16. T.C. Awes et al., Phys. Rev. Lett. **61**, 2665 (1988).
17. P.A. DeYoung et al., Phys. Rev. **C39**, 128 (1989).
18. D. Ardouin et al., Nucl. Phys. **A495**, 57c (1989).
19. P.A. DeYoung et al., Phys. Rev. **C41**, R1885 (1990).
20. D.H. Boal et al., Rev. Mod. Phys. **62**, 553 (1990).
21. W.G. Gong et al., Phys. Lett. **B246**, 21 (1990).
22. W.G. Gong et al., Phys. Rev. Lett. **65**, 2114 (1990).
23. W.G. Gong et al. Phys. Rev. **C43**, 781 (1991).
24. W.G. Gong et al., Phys. Rev. **C43**, 1804 (1991).
25. D. Goujdami et al., Z. Phys. **A339**, 293 (1991).
26. B. Erasmus et al. Phys. Rev. **C44**, 2663 (1991).
27. W. Bauer et al., Annu. Rev. Nucl. Part. Sci. **42**, 77 (1992).
28. D. Rebreyend et al., Phys. Rev. **C46**, 2387 (1992).
29. A weak signal of marginal statistical significance was reported in ref. [25].
30. G.D. Westfall et al., Nucl. Instr. and Meth., **A238**, 347 (1985).
31. W.G. Gong et al., Nucl. Instr. and Meth., **A268**, 190 (1988).

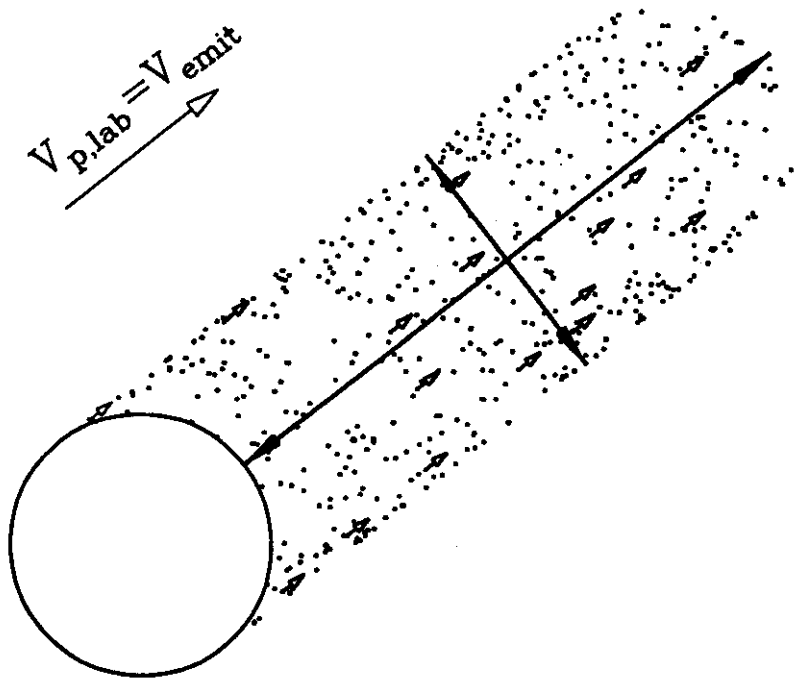
32. W.G. Gong et al., Nucl. Instr. and Meth., A287, 639 (1990).
33. G.F. Bertsch, Nucl. Phys. A498, 173c (1989).
34. M.A. Lisa et al., submitted to Phys. Rev. C.
35. L. Phair et al., Nucl. Phys. A548, 489 (1992)

Figure Captions:

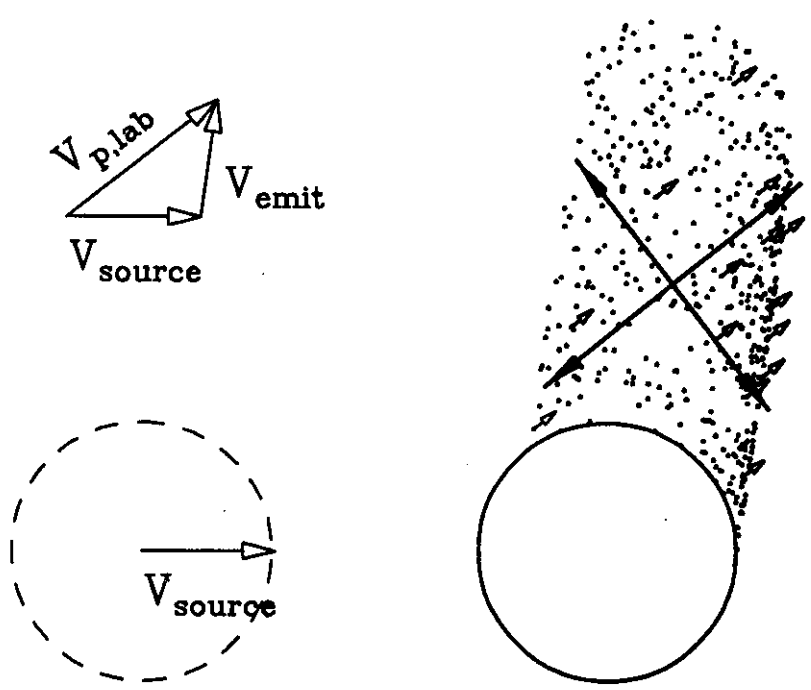
Fig. 1: Schematic illustration of phase space distributions at a time $t = 70 \text{ fm}/c$, seen by a detector at $\theta_{\text{lab}} = 38^\circ$, for a spherical source of radius $r = 3.5 \text{ fm}$ and lifetime $\tau = 70 \text{ fm}/c$ emitting protons of momentum $250 \text{ MeV}/c$. Part a: Source at rest in the laboratory. Part b: Source moves with $v_{\text{source}} = 0.18c$.

Fig. 2: Measured longitudinal and transverse correlation functions for protons emitted in central $^{36}\text{Ar} + ^{45}\text{Sc}$ collisions at $E/A = 80 \text{ MeV}$; the correlation functions are shown for proton pairs of total laboratory momenta $P=400\text{-}600 \text{ MeV}/c$ detected at $\langle\theta_{\text{lab}}\rangle=38^\circ$. Longitudinal and transverse correlation functions (solid and open points, respectively) correspond to $\psi = \cos^{-1}(\mathbf{q}\cdot\mathbf{P}/qP) = 0^\circ - 50^\circ$ and $80^\circ - 90^\circ$, respectively, where \mathbf{P} is defined in the rest frame of the presumed source. Upper panel: $v_{\text{source}} = 0.18c$; solid and dashed curves represent longitudinal and transverse correlation functions predicted for emission from a Gaussian source with $r_0 = 3.5 \text{ fm}$ and $\tau = 70 \text{ fm}/c$, moving with $v_{\text{source}} = 0.18c$. Lower panel: $v_{\text{source}} = 0$.

Fig. 3: Contour diagram of χ^2/ν (chi-squared per degree of freedom) determined by comparing theoretical correlations functions to the data shown in the upper panel of Fig. 2. The fit was performed in the peak region of the correlation function, $q = 15\text{-}30 \text{ MeV}/c$. Details are discussed in the text.



(a)



(b)

$^{36}\text{Ar} + ^{45}\text{Sc}; E/A = 80\text{MeV}; \langle \theta_{\text{lab}} \rangle = 38^\circ$

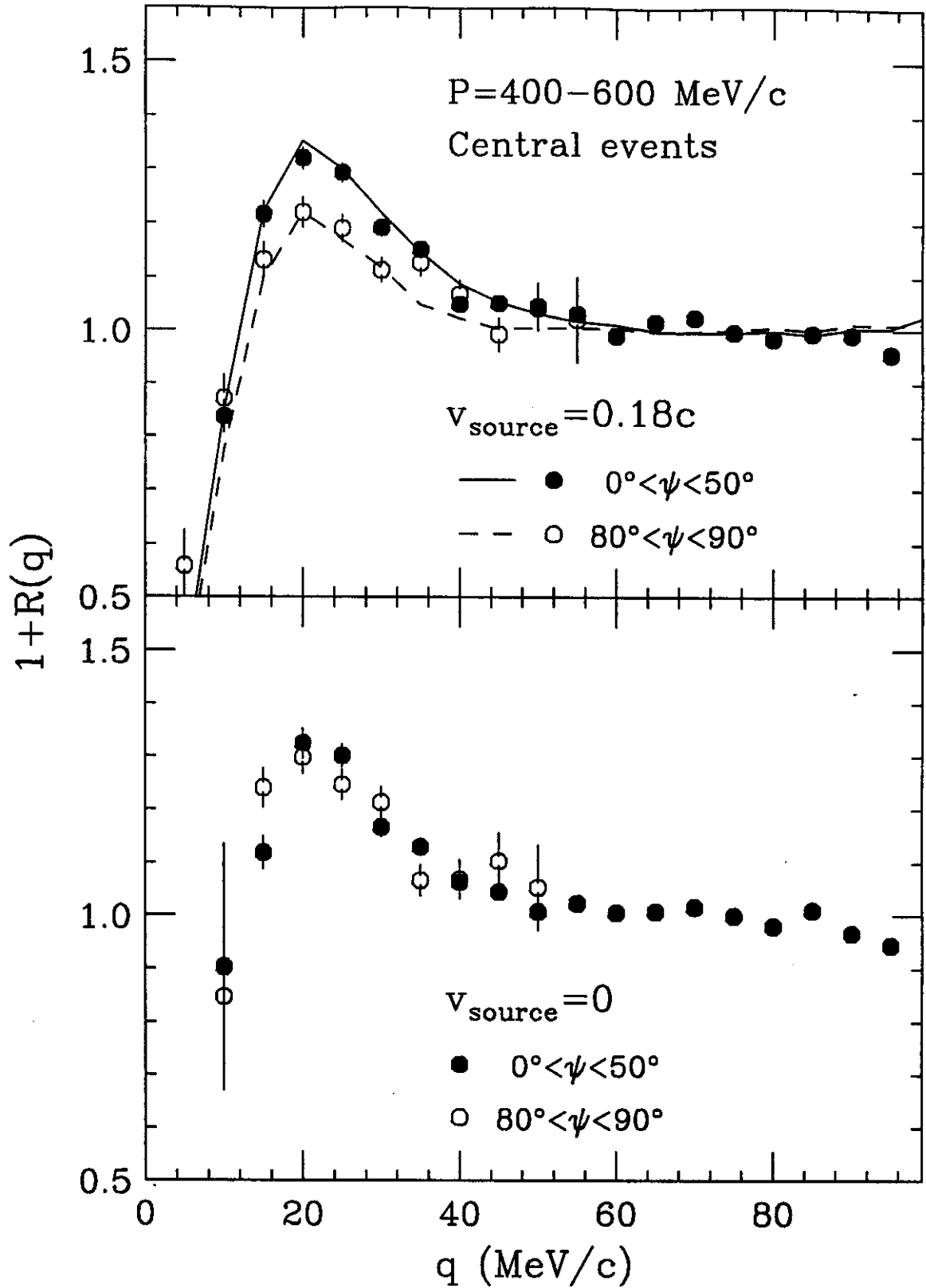


fig 2

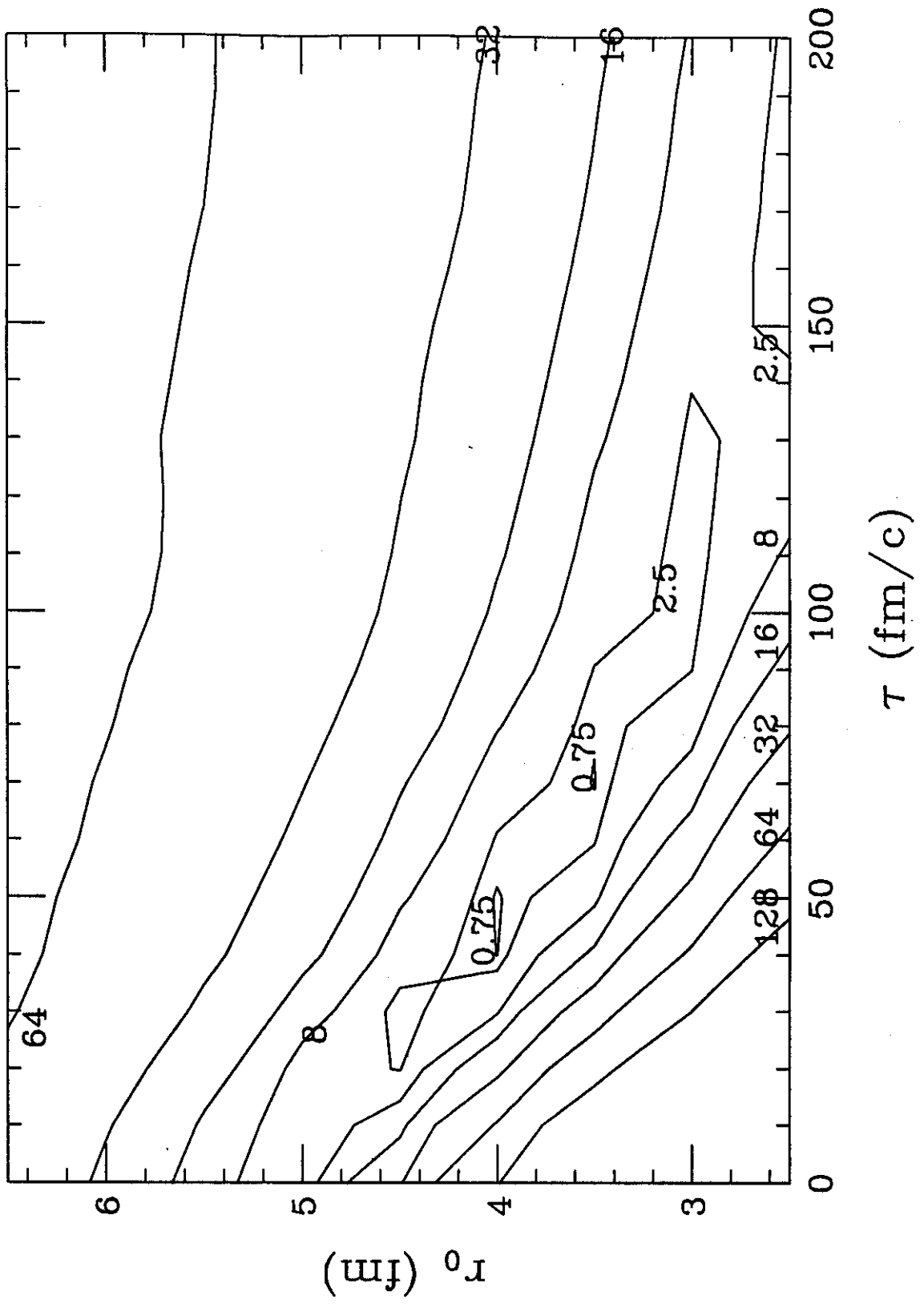


fig 3